Influence of mesoscale physical forcing on trophic pathways and fish larvae retention in the central Cantabrian Sea

RAFAEL GONZÁLEZ-QUIRÓS,[1,]* ANANDA PASCUAL,[2] DAMIÁ GOMIS[2] AND RICARDO ANADÓN[1]

[1]*Universidad de Oviedo, Dpto. Biología de Organismos y Sistemas (Área Ecología), c/Catedrático Rodrigo Uría s/n, 33071 Oviedo, Spain*
[2]*IMEDEA (UIB-CSIC), Cross-disciplinary Oceanographic Group, c/Miquel Marquès 21, 07190 Esporles, Mallorca, Spain*

ABSTRACT

This study was carried out over the central Cantabrian shelf during a post-bloom phase in May. Late phases of the spring phytoplankton bloom, which are characterized by high crustacean mesozooplankton biomass, have been proposed to be a particular case for high-energy flow towards large metazoans. The overall objective of the study is to analyse the influence of mesoscale physical forcing on primary production patterns, its implications on food web pathways, and on larval fish distribution during a period of intense spawning of *Sardina pilchardus* and *Scomber scombrus*. Physical and biological variables of different trophic levels show coupled cross-shelf and along-shelf heterogeneity. Quasi-geostrophic analysis and other indirect approaches, such as the depth of the slope salinity maximum, reveal predictable patterns of vertical instabilities associated with mesoscale physical forcing that enhance production of large-size phytoplankton. The latter is expected to enhance the energy flow towards higher trophic levels at a time of high mesozooplankton biomass. Distributions of *S. pilchardus* and *S. scombrus* eggs and larvae indicate retention related to the coastal salinity front and the overall eastward circulation pattern. The observed mesoscale physical processes may favour survival of early stages of fish by their influence on the energy flow of primary production towards higher trophic levels and larval retention at the coast.

Key words: canyon, food web, ichthyoplankton, mesoscale, physical–biological coupling, quasigeo strophy, slope current

**Correspondence*. e-mail: rafael@coast.ucsd.edu
Present addresses: Rafael González-Quirós, Integrative Oceanography Division, Scripps Institution of Oceanography, University of California, San Diego 0218, 9500 Gilman Dr, La Jolla, CA 92093-0218, USA.
Ananda Pascual, CLS Space Oceanography Division, 8–10 Rue Hermes Parc Technologique du Canal, 31526 Ramonville Saint-Agne, France.
Received 30 May 2002
Revised version accepted 17 December 2003

INTRODUCTION

Continental shelves are characterized by high primary production, important associated fisheries and intense pelagic fish spawning activity. This productivity and the distribution patterns of organisms present great spatial heterogeneity. It is suggested that the physical forcing that occurs within the mesoscale (scales of 10–100 km) is the ultimate cause of these characteristics in several shelf areas. Hypotheses on the factors that regulate survival of early life stages of fish, and controlling population recruitment variability (Cushing, 1996), refer to biological production (Cushing, 1975) and retention processes (Iles and Sinclair, 1982). Integration of both of these aspects, in view of their dependency on mesoscale physical forcing, has been shown to be an appropriate approach in particular cases (e.g. Checkley *et al*., 1988; Cury and Roy, 1989; Fortier *et al*., 1992).

Several mesoscale physical processes can influence primary productivity on continental shelves: coastal upwelling (Peterson *et al*., 1988), divergence between different water masses (Checkley *et al*., 1988), internal waves (Le Fèvre and Frontier, 1988), tidal currents (Le Fèvre, 1986) and the interaction between shelf currents or internal waves with topographic features such as canyons (Shea and Broenkow, 1982). Internal tidal waves result from the interaction of the barotropic surface tide with steep shelf break topography (Pingree *et al*., 1986) and are associated with physical mixing of the water column and upwelling of nutrients (New and Pingree, 1990). Topographic canyons are preferential sites of exchange between the shelf and the slope. These exchanges can have important implications for the structure and dynamics of the planktonic communities and the productivity of coastal areas (e.g. Denman and Powell, 1984).

Nevertheless, primary production in temperate areas is mostly governed by the seasonal pattern of segregation between nutrients and light. Although fish production is ultimately dependent on total primary production on a global scale (Pauly and Chirstensen, 1995), the energy flow towards high trophic levels (fish) also depends on the degree of match between large size primary production and crustacean mesozooplankton grazing (Legendre and Rassoulzadegan, 1996). In temperate areas, this flow is limited by the temporal lag between maximum primary production and maximum abundance of mesozooplankton in spring. Legendre and Rassoulzadegan (1996) proposed that late phases of the phytoplankton spring bloom, when crustacean mesozooplankton biomass has already increased, are a particular case in which the flow towards higher trophic levels would be particularly high. Shelf-related mesoscale processes occurring during late, post-bloom phases may interact with the seasonal productivity pattern and increase the temporal persistence of high production by large-sized phytoplankton, therefore enhancing energy flow towards higher trophic levels, including fish larvae. In addition, shelf-break fronts are closely related to ichthyoplankton distribution (Sabatés and Masó, 1990; Munk *et al.*, 1995) and their physical dynamics have been proposed as important factors on the recruitment of several species (Checkley *et al.*, 1988; Koutsicopoulos *et al.*, 1991).

The present study analyzes the role of mesoscale physical dynamics in the survival of fish in their early stages in the central Cantabrian Sea, at a time when the spring bloom has already occurred and nutrient concentration in the surface layer is low. In this area, the spring phytoplankton bloom occurs in April (Fernández and Bode, 1991) and high mesozooplankton biomass is observed in May (M. Llope, Universidad de Oviedo, personal communication), when copepods comprise more than 80% by number of the mesozooplankton. Highest ichthyoplankton abundance occurs in spring, and it is dominated by *Sardina pilchardus* (sardine), *Scomber scombrus* (mackerel) and *Trachurus trachurus* (horse mackerel) (González-Quirós, 1999). In spring, the most conspicuous hydrographic feature in the Cantabrian Sea is a high salinity water mass that has been observed both in March (Fernández *et al.*, 1993) and April (Fernández *et al.*, 1991), and which is linked to a poleward slope current of relatively saline waters (Frouin *et al.*, 1990; Haynes and Barton, 1990). Fernández *et al.* (1991) suggest a

Figure 1. Area of study, including the bathymetry and the sampling grid. T1–T7, Transects 1–7. Selected stations along T3 and T6 are marked within a square. These stations are classified as coastal (18, 41), mid-shelf (32, 46) and slope (23, 44). Station numbers refer to the sequence of sampling.

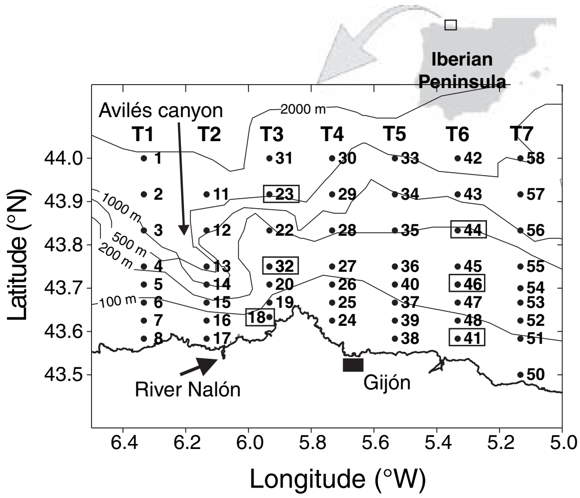

system based on the microbial food web at the saline intrusion in contrast with a classical food chain in coastal and oceanic water masses. Frontal systems associated with the high salinity water mass influence the distribution of chlorophyll, primary production, neritic plankton and ichthyoplankton (Fernández *et al.*, 1993). Another feature worth noting is the high primary production observed in May at the southern edge of the Avilés canyon (within the study area, Fig. 1), which seems to be related to a dome-shaped feature in the cross-shelf vertical distribution of density and with the distribution of eggs of sardine, mackerel and horse mackerel (González-Quirós *et al.*, 2003).

In this work, we infer vertical velocities from quasi-geostrophic (QG) theory, as well as identifying some limitations of the QG framework from other indirect evidence. We present a multitrophic data set including size-fractionated chlorophyll *a* concentration and primary production and mesozooplankton and ichthyoplankton distributions. The specific objectives in this study are to: (1) identify and characterize mesoscale physical structures and their associated vertical velocity instabilities; (2) analyse the role that these processes have on different size fractions of primary producers; and (3) investigate the relation of mesozooplankton and ichthyoplankton distributions to the physical structure and productivity patterns, in order to infer about possible consequences on retention of and food availability for fish early stages.

MATERIALS AND METHODS

All results presented in this work have been obtained from the data collected during an intensive oceanographic survey (SARDINA) in the central Cantabrian shelf slope. The surveyed domain is characterized by a roughly 30-km wide continental shelf indented by a steep canyon on the western part of the domain (Fig. 1). The survey took place from May 2 to May 11, 2000 and was carried out on board R/V *Garcia del Cid*. CTD casts with a calibrated fluorometer and bongo net tows were made at 60 stations distributed along seven transects perpendicular to the coast (Fig. 1). The mean distance between transects was about 15 km, and the distance between stations along transects ranged from 5 km near the shore to 10 km over the shelf edge (see Fig. 1). Zooplankton and ichthyoplankton abundances were estimated from the bongo net samples.

The vertical distribution of nitrate concentration was measured in each station along Transects 3 and 6 (Fig. 1). Chlorophyll *a* concentration and primary production were measured and estimated from water samples at three stations in both transects, located close to the coast, at mid-shelf and at the slope (see Fig. 1).

The hydrodynamical data set

Hydrodynamical variables (temperature, salinity and density) and fluorescence were interpolated from observation points onto grid points using a successive correction scheme with weights normalized in the 'observation space' (Bratseth, 1986). The horizontal and vertical characteristic scale parameters were set to 20 km and 20 m, respectively, according to correlation statistics. Normal-error filter convolution was applied (Pedder, 1993), in order to filter out scales that could not be resolved by the sampling. The cut-off wavelength was set to 30 km in the horizontal and 30 m in the vertical.

The biochemical data set

Water samples obtained from Niskin bottles mounted on a rosette were used to measure nitrate, chlorophyll *a* and primary production. At least five samples were taken from the euphotic layer, always including 100 and 1% of incident light and the fluorescence maximum. Deeper samples, only for nutrient and chlorophyll *a* concentration, were taken at increasing intervals.

Nitrate concentration was measured with a Technicon Autoanalizer II (Grasshoff *et al.*, 1983). Chlorophyll *a* concentration of >5-μm and 0.2–5-μm fractions was estimated by filtering 200 mL of sea water sequentially through 5- and 0.2-μm polycarbonate filters that were immediately frozen and stored at −20°C. Chlorophyll *a* was measured fluorometrically after extraction in 90% acetone for 24 h at 4°C (Strickland and Parsons, 1972). Primary production was estimated in the euphotic layer using the ^{14}C method. Three replicates of 125 mL were inoculated with 10 μC_i of $NaH^{14}CO_3$, and incubated for 2 h at the temperature of the fluorescence maximum and irradiance that simulated *in situ* conditions. Temperatures at the fluorescence maximum were 12.7–13.9°C and temperatures within the euphotic layer were 12.5–15.5°C. Subsequently, samples were fractionated as for the chlorophyll *a*. Radioactivity was measured in a Packard liquid scintillation counter, after addition of Optiphase Hi-safe scintillation liquid.

Zooplankton and ichthyoplankton were sampled with a 60-cm-diameter bongo net with 200-μm-mesh nets and calibrated flowmeters. Bongo tows were to a depth of 150 m or to 5 m above the bottom, whichever was less. Ship speed during bongo tows was maintained at 1 m s^{-1}. Samples were preserved with buffered formaldehyde. Most adult and CV copepods were identified to species, and most of the remaining copepodids to genera. Other zooplankton groups were identified to different taxonomic levels. In this study we present data of the abundance of total copepods and total appendicularians, copepodids I–IV of a group of species called Calanidae I, which includes *Calanus* sp., *Calanoides* sp. and *Neocalanus* sp., adult and copepodid *Acartia clausii*, adults and copepodid *Centropages* sp. and adult *Pseudocalanus elongatus*. In regard to ichthyoplankton, only the abundances of eggs and larvae of *Sardina pilchardus* and *Scomber scombrus* are reported.

Computation of Quasi-Geostrophic Dynamics

Dynamic height (the vertical integration of specific volume anomaly above a level of no motion) is computed from station density profiles and then interpolated onto grid points. It is worth noting that dynamic height is defined with respect to a reference level assumed to be of no motion. However, the selection of a deep reference level in shelf/slope regions is handicapped by the fact that dynamic height cannot be computed for CTD profiles shallower than the reference depth. We therefore chose 500 m as a compromise reference level. Derived dynamical variables, such as geostrophic velocity or geostrophic vorticity, are then obtained from grid point values of dynamic height by finite differences. We derive vertical velocity, w, by integrating the Q-vector form of the QG

Figure 2. Distributions of temperature (°C; a), salinity (b) and σ_t (kg m^{-3}; c) at 15-m depth. Bold line corresponds to the 500-m isobath. T1–T7, Transects 1–7.

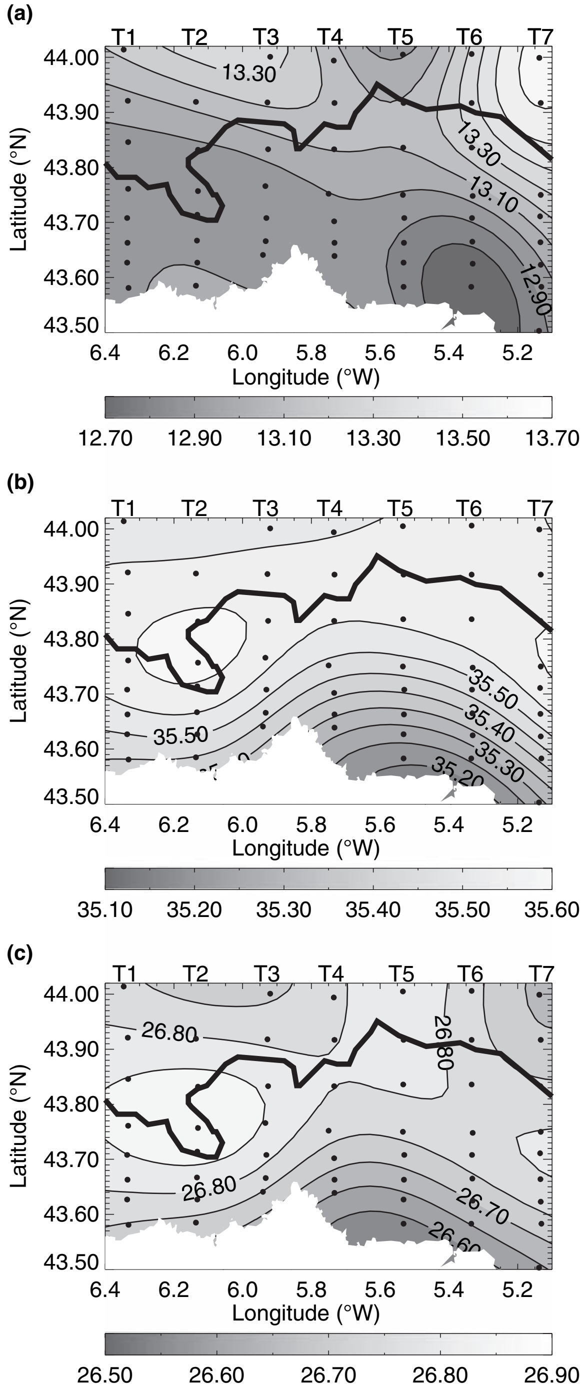

Figure 3. As for Fig. 2, at 55 m depth and only for temperature (a) and salinity (b).

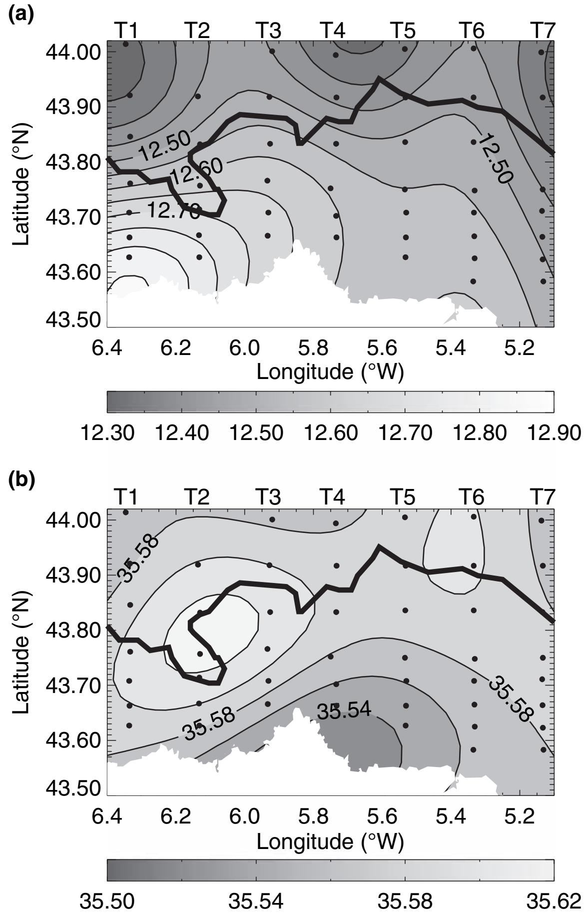

omega equation (Hoskins *et al.*, 1978). This is integrated setting $w = 0$ at the upper and lower boundaries and setting its normal derivative to zero at the lateral boundaries (Pinot *et al.*, 1996).

RESULTS

Main Features of Hydrographic Distributions

Over the shelf, both temperature and salinity gradients were mostly perpendicular to the shore. Salinity distributions always showed fresher water near the coast, with cross-shelf differences reaching 0.3 in upper levels (Fig. 2b) and decreasing with depth (less than 0.1 at 55 m, Fig. 3b). A coastal nucleus of cold water (temperature values almost 1°C lower than the surroundings) dominated the upper 30 m (Fig. 2a). Deeper, the temperature field was dominated by large-scale cross-shelf gradients (0.5°C), with warmer water near the coast (Fig. 3a). Over and offshore of the shelf break (i.e. in the northern half of the domain covered by the cruise), salinity and, especially, temperature and density were characterized by pronounced meandering (Fig. 2). A salinity maximum existed over the shelf break, especially marked over the canyon (Fig. 2b).

Figure 4. Distributions of dynamic height (DH; grey scale) and superimposed geostrophic velocity (arrows) at 15 m (a) and quasi-geostrophic (QG) vertical velocity at 105 m (b). Units are dyn cm for DH and m day^{-1} for QG vertical velocity. Maximum horizontal velocity is 6 cm s^{-1}. Bold line and T1–T7 as in Fig. 2.

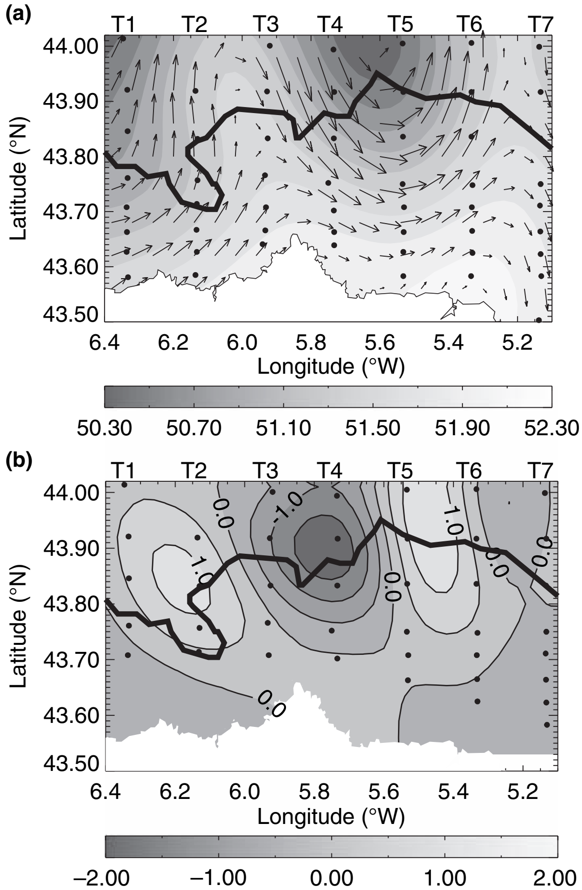

Inferred 3D QG Circulation

Dynamic height reflects the meandering structure over the shelf edge (Fig. 4a). The flow was deflected offshore, with a cyclonic curvature, when it passed over the canyon, and an anti-cyclonic meander downstream of the canyon and a more intense cyclonic meander later on. The maximum geostrophic velocity was ~6 cm s^{-1}, at the meandering frontal structure (Fig. 4a).

The vertical velocity field (Fig. 4b) is consistent with the described meandering pattern, with maximum upward velocities obtained in regions where cyclonic vorticity is advected by the mean flow. This happens downstream of cyclonic gyres, which in our domain means over the eastern wall of the canyon (Transect 2) and over Transect 6. Maximum vertical velocities are of the order of 1.5 m day^{-1}.

However, actual upwelling rates could be substantially higher, as inferred from other evidence, e.g. looking at the saline intrusion along different transects (Fig. 5). Waters of salinity more than 35.64 were seen to flow over the slope (125–150 m) just before impinging onto the canyon (Fig. 5a). Over the canyon they were markedly deflected offshore and lifted up to less than 50 m depths (Fig. 5b). According to the horizontal distance along which the upwelling took place (15 km) and to the horizontal velocities (~6 cm s^{-1}), waters would have been upwelled at a rate of about 30 m day^{-1}, i.e. more than one order of magnitude higher than the diagnosed QG vertical velocities. This provides evidences for a significant topographic (non-geostrophic) vertical forcing linked to the steepness of the canyon walls. From Transect 2 (Fig. 5b) to Transect 5 (Fig. 5c), the intrusion remained at about the same depth, while from Transect 5 to 6 (Fig. 5d) the intrusion was again lifted from about 40 m to about 25 m, coinciding with the second maximum of the QG vertical velocity (Fig. 4b). In this case, the inferred upwelling rate would be of the order of 5 m day^{-1}.

Phytoplankton and Nitrate

At the time the survey was conducted, nitrate concentration was low in the upper layers (Fig. 6). The vertical distribution of chlorophyll *a* showed a subsurface maximum at the nutricline (Fig. 7), the depth of which was 13–30 m at stations with >1 mg chl *a* m^{-3}. Vertical distribution of primary production presented a similar pattern (data not shown).

Integrated chlorophyll *a* and chlorophyll *a* concentration at 15 m (Fig. 8) were positively correlated with salinity and σ_t at 15 and 55 m (Table 1). Higher integrated chlorophyll *a* was observed along the shelf edge (Fig. 8a), matching with the along-slope salinity maximum and decreasing eastward. Two chlorophyll *a* maxima at 15 m were observed at the shelf edge (Fig. 8b), co-located with the diagnosed upward QG vertical velocities. Of these, the highest fluorescence values were obtained over the canyon, in agreement with the higher upward velocities inferred from the vertical displacement of the salinity maximum (but not with the lower QG vertical velocity values).

Vertical distribution of nitrate along Transects 3 and 6 (Fig. 6) showed differences offshore which are also consistent with the vertical velocity field (Fig. 4b): in Transect 6 (upward vertical velocities), the nitracline was shallower than in Transect 3 (downward vertical velocities). For both transects, the distribution of nutrients presented a dome-shaped

Figure 5. Vertical cross-sections of the salinity field along Transects 1 (a), 2 (b), 5 (c) and 6 (d).

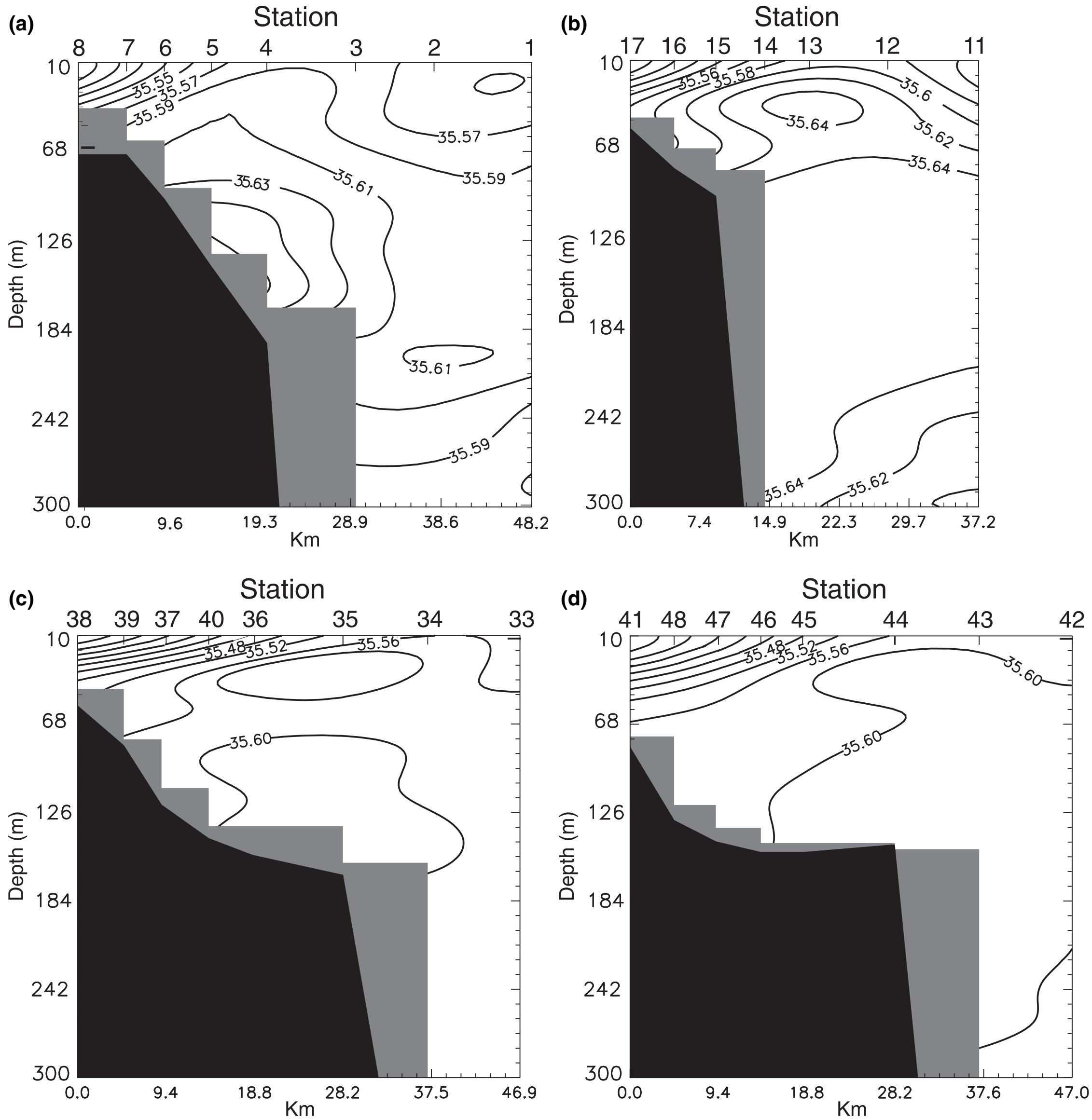

feature over the shelf (higher concentrations in the euphotic layer). Finally, high nutrient concentration in the upper layer was also observed at the closest station to the coast in Transect 3, perhaps influenced by the Nalón river runoff.

Phytoplankton biomass was dominated by the >5 μm size fraction (L) at the mid-shelf and coastal stations, whereas the <5 μm fraction (S) dominated at slope stations (Table 2), located within the saline intrusion (Fig. 2b). The relative importance of the L fraction (L/T, Table 2) is significantly higher at the coastal and mid-shelf stations than at slope stations (ANOVA, $N = 6$, $F = 26.29$, $P = 0.01$; Scheffé test, $P = 0.02$ in both cases). Primary production showed a similar pattern, although there was only a significant difference between mid-shelf and slope stations (ANOVA, $N = 6$, $F = 12.20$, $P = 0.04$; Scheffé test, $P = 0.03$). Highest production of L was observed at mid-shelf stations (Table 2), coincident with the dome-shaped feature observed in the nutrient distribution. However, there were only significant differences between mid-shelf and slope stations (ANOVA, $N = 6$, $F = 15.76$, $P = 0.03$; Scheffé test, $P = 0.03$). Although both slope stations had similar phytoplankton biomass, primary production was higher in Transect 6 (Table 2), consistent with upward velocities and the

Figure 6. Vertical distribution of nitrate concentration along Transects 3 (a) and 6 (b). Units are μM.

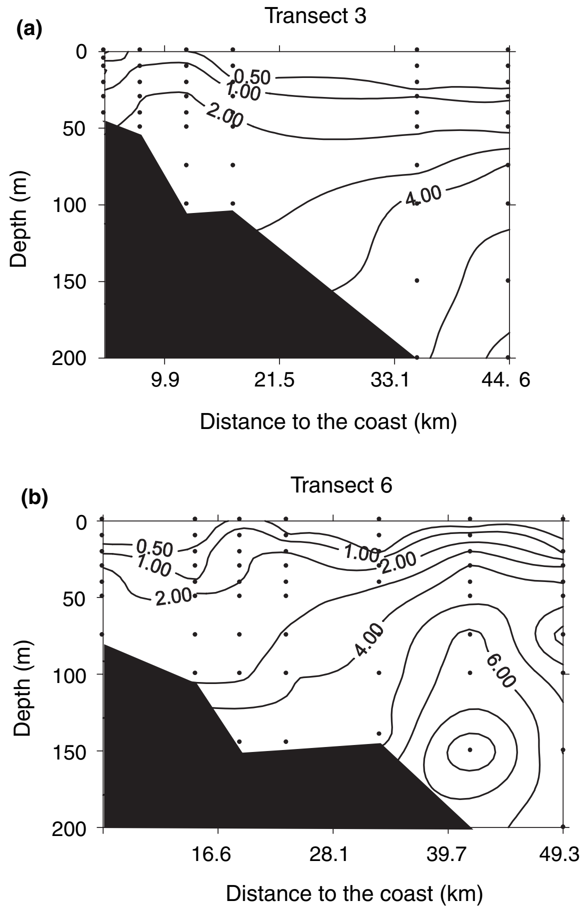

Figure 7. Vertical distribution of >5 μm (circles and continuous line) and 0.2–5 μm (triangles and dashed line) chlorophyll *a* concentration at slope (a, b), mid-shelf (c, d) and coastal stations (e, f) in Transects 3 (a, c, e) and 6 (b, d, f). Units are mg chl *a* m^{-3}. D.c., distance to the coast in km.

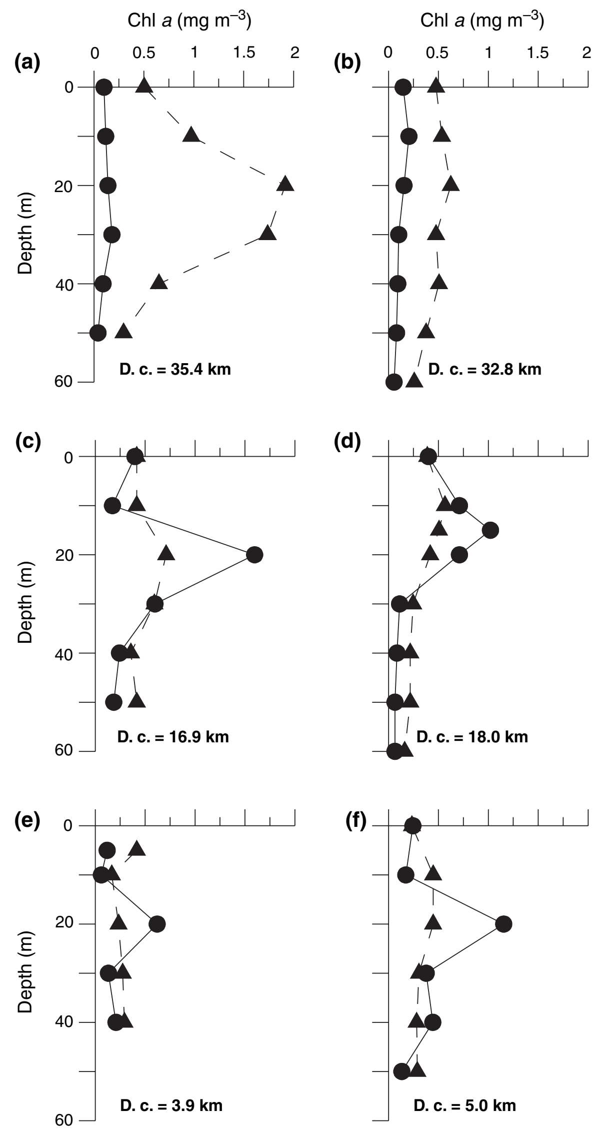

shallower nitracline. Moreover, *photosynthetic efficiency* (PP/chl *a*; total and for both size fractions) was within the range found at coastal stations, and the relative importance of L production was intermediate between values observed at the shelf stations (coastal and mid-shelf) and the slope station in Transect 3.

Zooplankton and Ichthyoplankton Distributions

Copepod (>200 μm) mean abundance was 7086 individuals m^{-3} (SD 4081), which represented 89% (SD 8.8%) of the total mesozooplankton ($N = 54$). Abundance was greater over the shelf (Fig. 9a) and negatively correlated with temperature and salinity (Table 3). Calanidae I CI-CIV copepodites (Fig. 9c), *Acartia clausi* (Fig. 9d), *Centropages* sp. (Fig. 9e) and *Pseudocalanus elongatus* (Fig. 9f) occurred in high concentrations over the shelf. Their abundance was more strongly correlated with physical variables than total copepod abundance (Table 3). Appendicularians (Fig. 9b) were negatively correlated with salinity, σ_t and chlorophyll *a* and had a similar distribution pattern to the copepods over the shelf. However, their offshore distribution resembled the meandering circulation; high abundance coincided with the observed cyclonic gyre in the centre of the survey domain and low abundance was observed in Transects 2 and 6, where dynamic height indicated offshore transport (Fig. 4a).

Larvae and eggs of sardine and mackerel comprised 43 and 22% of total larvae and 36 and 22% of total

Figure 8. Distributions of integrated chlorophyll a (mg chl *a* m^{2}; a) and chlorophyll a concentration at 15 m (mg chl *a* m^{-3}; b). Bold line and T1–T7 as in Fig. 2.

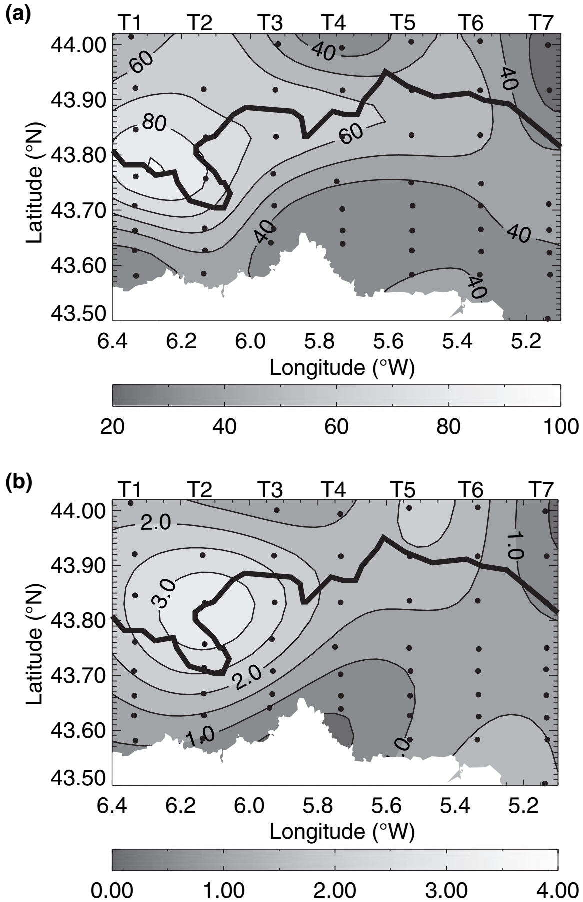

eggs, respectively. The distribution of sardine eggs suggests active spawning very close to the coast (Fig. 10a). Sardine larva distribution indicated higher offshore dispersion, although limited to over the continental shelf (Fig. 10c). Abundance of sardine eggs and larvae were negatively correlated with physical variables and chlorophyll *a* (Table 3), except with temperature at 55 m (positive correlation), which is related to the opposing cross-shelf gradient of temperature at 15 and 55 m (Figs 2 and 3). Conversely, sardine eggs and larvae are positively correlated with all the mesozooplankton groups included herein (Table 4). The distribution of mackerel eggs exhibited two distinct areas with high abundance: over the shelf and offshore (Fig. 10b). A low abundance area in between coincided with the presence of the high salinity water mass. Mackerel eggs were only correlated significantly with salinity at 55 m (Table 3). Offshore, the egg distribution reflected the meandering circulation pattern, which is similar to the offshore distribution of appendicularians, the only mesozooplankton group positively correlated with mackerel eggs (Table 4). The pattern of mackerel larvae (Fig. 10d) was similar to that observed for sardine larvae, although the correlation with mesozooplankton groups is lower (Table 4).

DISCUSSION

The salinity nucleus observed along the shelf edge is characteristic of the high-salinity slope current (Frouin *et al.*, 1990; Haynes and Barton, 1990; Fernández *et al.*, 1991). Its eastward circulation pattern in our study is in agreement with previous observations in the Cantabrian Sea (Pingree and Le Cann, 1990). This current causes onshelf entrapment of low salinity coastal waters (e.g. Fernández *et al.*, 1993). Our study reveals an along-slope meandering mesoscale circulation, which causes heterogeneity in the vertical velocity field. Furthermore, using the salinity nucleus as a tracer of the slope current, we infer that higher upwelling velocities were associated with the Avilés Canyon. In this context, physical and biological variables from different trophic levels show coupled cross-shelf and along-shelf heterogeneity, namely: (1) high integrated chlorophyll *a* is coincident with

Table 1. Spearman *R* correlation coefficient (non-parametric) of physical variables (temperature, °C; salinity; σ_t, kg m^{-3}) at 15 and 55 m with integrated chlorophyll *a* (mg chl *a* m^{-2}) and concentration of chlorophyll *a* (mg chl *a* m^{-3}) at 15 m.

	Physical variable					
	Temperature		Salinity		σ_t	
Depth	15 m	55 m	15 m	55 m	15 m	55 m
Integrated chl *a*	0.29*	0.06	0.68**	0.74**	0.72**	0.36*
Chl *a* 15 m	0.08	0.05	0.55**	0.74**	0.73**	0.38**

*P < 0.05; **P < 0.01. $N = 53$ and $N = 47$ for correlation with physical variables at 15 and 55 m, respectively.

Table 2. Integrated chlorophyll *a* (chl *a* mg m^{-2}), integrated primary production (mg C m^{-2} h^{-1}) and PP/chl *a* index (h^{-1}) at slope, mid-shelf and coastal stations in Transects 3 and 6.

	Transect 3				Transect 6			
Station	T	S	L	L/T	T	S	L	L/T
Integrated chl *a*								
Slope	41.8	36.4	5.3	0.13	21.1	14.8	6.3	0.30
Mid-shelf	40.0	13.1	26.9	0.67	27.2	8.3	18.9	0.69
Coast	15.3	5.4	9.9	0.65	28.7	8.2	20.5	0.71
Integrated PP								
Slope	28.4	24.3	4.2	0.15	83.9	49.8	34.1	0.41
Mid-shelf	231.9	39.5	192.5	0.83	190.1	36.9	153.2	0.81
Coast	71.1	21.3	49.9	0.70	114.0	17.3	96.7	0.84
PP/chl *a* index								
Slope	0.68	0.66	0.79		3.99	3.37	5.43	
Mid-shelf	5.81	3.02	7.16		6.99	4.43	8.11	
Coast	4.65	3.94	5.03		3.98	2.11	4.72	

Chl *a*, chlorophyll *a*; PP, primary production; T, total phytoplankton; S, 0.2 –5 μm phytoplankton; L, >5 μm phytoplankton.

Table 3. Spearman *R* correlation coefficient (non-parametric) of physical variables (temperature, °C; salinity; σ_t, kg m^{-3}) at 15 and 55 m, integrated chlorophyll *a* (mg chl *a* m^{-2}) and concentration of chlorophyll *a* (mg chl *a* m^{-3}) with the abundance (no. m^{-3}) of several meso- and ichthyoplankton groups. CI–CIV Calanidae I includes copepodites I–IV of *Calanus* sp., *Calanoides* sp. and *Neocalanus* sp.; *Acartia clausi*, and *Centropages* sp. include adult and copepodites; and *Pseudocalanus elongatus* only adults and copepodites V.

	Physical variable							
	Temperature		Salinity		σ_t		Chl *a*	
Depth	15 m	55 m	15 m	55 m	15 m	55 m	Integrated	15 m
Total copepods	−0.31*	−0.17	−0.39**	−0.11	−0.23	−0.22	−0.05	−0.02
Appendicularians	−0.25	0.09	−0.48**	−0.46**	−0.28*	−0.36*	−0.45**	−0.42**
CI–CIV Calanidae I	−0.45**	0.48**	−0.55**	−0.17	−0.38**	−0.53**	−0.38**	−0.24
Acartia clausi	−0.34*	0.23	−0.40**	−0.09	−0.31*	−0.24	−0.05	0.01
Centropages sp.	−0.59**	0.68**	−0.61**	−0.28	−0.32*	−0.77**	−0.37**	−0.32*
Pseudocalanus elongatus	−0.58**	0.48**	−0.60**	−0.28	−0.26	−0.65**	−0.42**	−0.37**
Sardina pilchardus eggs	−0.48**	0.56**	−0.61**	−0.37*	−0.54**	−0.68**	−0.52**	−0.36**
Scomber scombrus eggs	−0.25	−0.00	−0.18	−0.40**	−0.05	−0.18	−0.22	−0.19
Sardina pilchardus larvae	−0.72**	0.59**	−0.80**	−0.54**	−0.46**	−0.83**	−0.57**	−0.44**
Scomber scombrus larvae	−0.42**	0.62**	−0.29*	−0.22	−0.06	−0.59**	−0.18	−0.09

*$P < 0.05$; **$P < 0.01$. $N = 53$ and $N = 47$ for correlation with physical variables at 15 and 55 m, respectively.

the along-slope distribution of the maximum salinity nucleus; (2) the distribution of several mesozooplankton groups and mackerel and sardine larvae are shown to follow the cross-shelf salinity gradient; (3) the circulation and the inferred vertical velocity field along the shelf edge are related to chlorophyll *a*, the nitracline depth, primary production and the distribution of appendicularians and mackerel eggs; and (4) the dome-shaped nutrient feature observed at mid-shelf stations, is related to high primary production rates dominated by large-size phytoplankton.

The main limitation of the QG computations is probably the missing non-geostrophic topographic forcing. This would explain why there is a severe underestimation of the ascent rates near the canyon. Other sources of errors that could affect the estimation of vertical velocity are observational errors (e.g. discrete sampling) and our use of 500 m as the reference level. These errors could also explain the underestimation of the rising motion in Transect 6.

Submarine canyons are effective topographic features that can induce flow modification, such as

Figure 9. Mesozooplankton distributions: total abundance of copepods (a), appendicularians (b), CI–CIV Calanidae I (includes *Calanus* sp., *Calanoides* sp. and *Neocalanus* sp.) (c), adult and copepodites of *Acartia clausi* (d), adults and copepodites of *Centropages* spp. (e) and adult *Pseudocalanus elongatus* (f). Units are individuals m^{-3}. T1–T7, Transects 1–7.

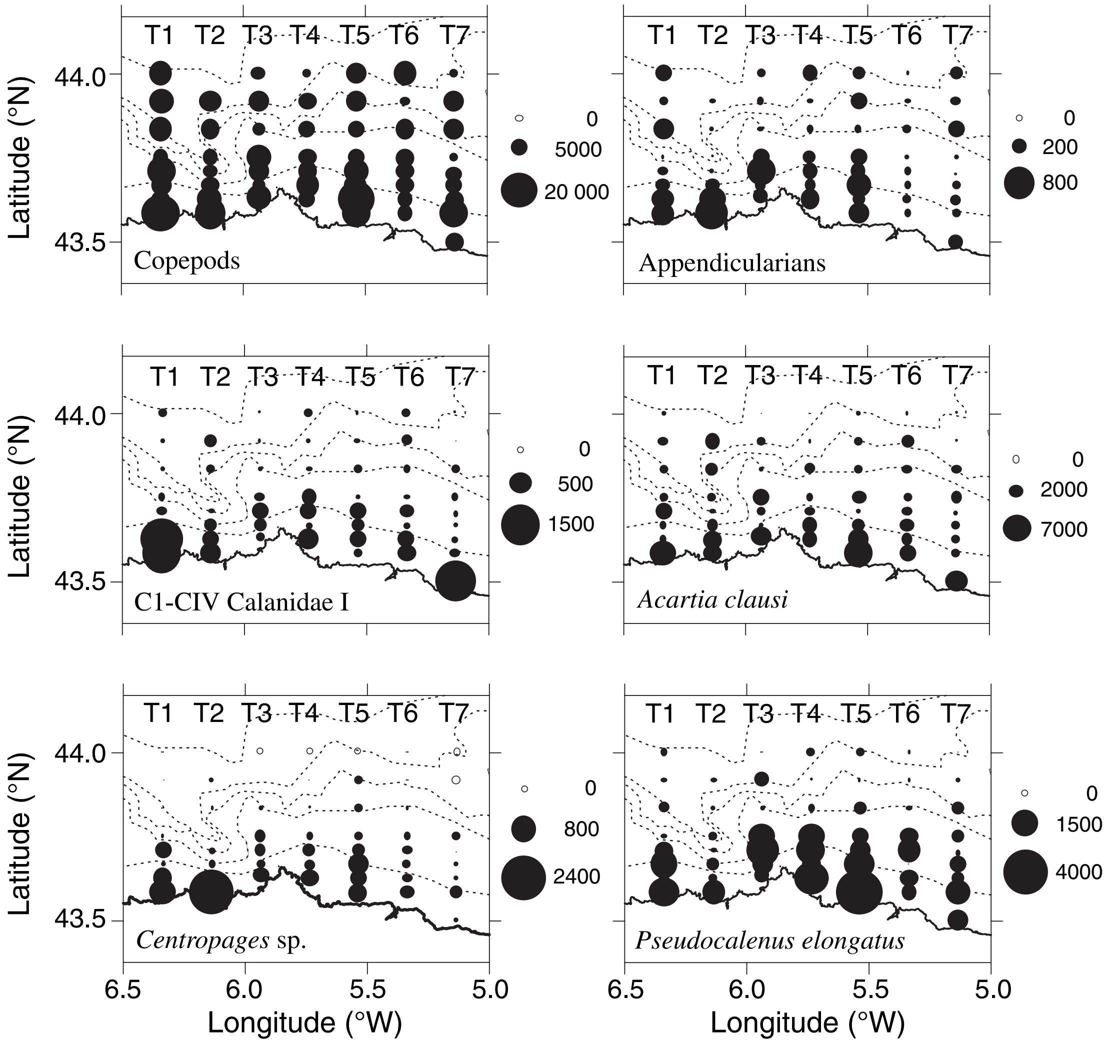

shelf-slope exchange and formation of meanders and eddies (Hickey, 1995; Alvarez *et al*., 1996). The first cyclonic meander, observed at the downstream wall of the canyon, could be due to the presence of the canyon, while the second meander could be part of some instability that might be propagating and/or growing/decaying. Gil *et al*. (2002) observed eddies propagating westward at velocities of about 2 km day^{-1} in the Cantabrian Sea, which is consistent with theoretical estimates of the phase speed of long non-dispersive Rossby waves. While other causes of the observed circulation pattern are possible, our results highlight the importance of bathymetrically mediated instabilities to coastal ecology and fisheries.

High integrated chlorophyll *a* at the shelf break coincides with the distribution of the along-slope salinity maximum. Highest chl *a* values are observed at the west of the survey domain, decreasing eastward. Mesoscale studies in coastal upwelling systems have shown that high phytoplankton biomass is displaced offshore (Peterson *et al*., 1988) and downstream in the alongshore current (Wieters *et al*., 2003) with respect to areas of maximum upwelling. Here, the pattern of phytoplankton biomass distribution may be, at least partially, a consequence of advection associated with the high salinity slope current from the west of the survey domain. Nevertheless, two maxima of chlorophyll *a* concentration at 15 m (the upper limit of the subsurface chlorophyll *a* maximum) coincide with the

Figure 10. Horizontal distributions of eggs and larvae of *Sardina pilchardus* (a, c) and *Scomber scombrus* (b, d). Units are eggs $(10\ m^3)^{-1}$ (a, b) or larvae $(10\ m^3)^{-1}$ (c, d). T1–T7, Transects 1–7.

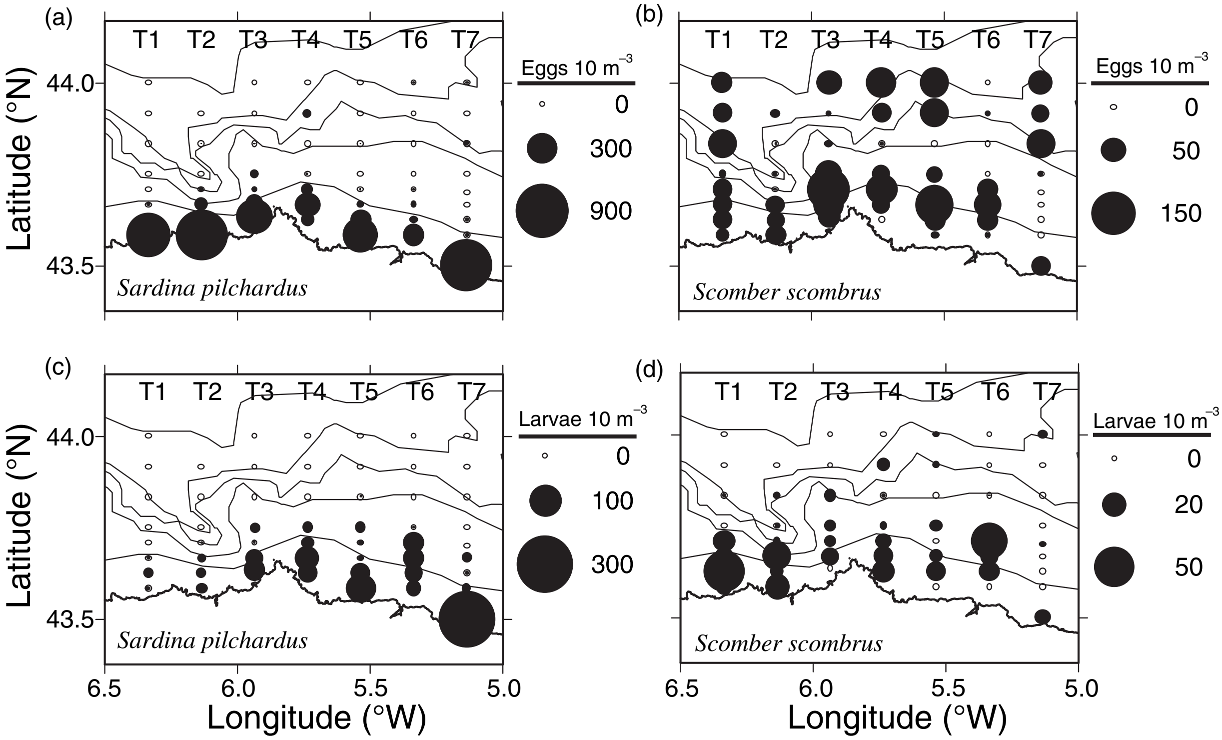

Table 4. Spearman *R* correlation coefficient (non-parametric) of the abundance (no. m^{-3}) of several mesozooplankton groups (as in Table 3) with the abundance (no. m^{-3}) of *S. pilchardus* and *S. scombrus* eggs and larvae.

	S. pilchardus		S. scombrus	
Mesozooplankton group	Eggs	Larvae	Eggs	Larvae
Total copepods	0.36**	0.33*	0.19	0.21
Appendicularians	0.46**	0.41**	0.60**	0.37**
CI-CIV Calanidae I	0.64**	0.60**	0.14	0.39**
Acartia clausi	0.40**	0.44**	0.03	0.20
Centropages sp.	0.66**	0.73**	0.11	0.46**
Pseudocalanus elongates	0.51**	0.64**	0.13	0.32*

$^*P < 0.05$; $^{**}P < 0.01$. $N = 53$.

diagnosed upwelling associated with the meandering circulation and the canyon topography. We assume that the elevation of the subsurface chlorophyll *a* maximum bears enhanced primary production. However, our limited observations prevented a quantification of this effect. High phytoplankton biomass was previously observed over the canyon in March (Fernández *et al.*, 1993), April (Fernández *et al.*, 1991) and May (González-Quirós *et al.*, 2003), which suggests a persistent influence of the canyon on primary production.

Dominance of large phytoplankton over the coast and mid-shelf, in contrast to the dominance of small phytoplankton at the high salinity slope current, suggests the existence of different communities of primary producers. Bode *et al.* (1990) and Fernández *et al.* (1993) used distributions of seston size, nutrients and phytoplankton composition to argue that regenerative processes associated with the microbial loop were more important at the saline intrusion than in adjacent coastal and oceanic water masses, where the classical food chain prevailed. Our limited results suggest covariance between water masses and food web pathways later in the season. However, differences in primary production related to the dome-shaped nitrate distribution and the offshore vertical velocity field appear to modify with this general pattern, as follows. (1) The dome-shaped feature is apparently related to high primary production rates over the shelf, where large-size phytoplankton was dominant. These rates are similar to the values observed by González-Quirós *et al.* (2003) at the edge of the Avilés Canyon in May, which were related to the presence of a similar dome-shaped feature in the distribution of density. In both cases, primary production was similar to maximum values observed during the spring bloom in the Cantabrian Sea earlier in the season (Fernández and Bode, 1991). It is known (e.g. Pingree *et al.*, 1986; New and Pingree, 1990) that, in the Bay of Biscay, tidal displacements of the seasonal thermocline occur with relatively large amplitudes near the shelf break and are associated with physical mixing and upwelling. It is possible that the dome-shaped nutrient distributions could be related to a similar physical mechanism. However, this hypothesis cannot be tested with the available data. (2) Primary production of large phytoplankton seems to be enhanced at the slope station where upward velocities are observed. Production of large phytoplankton might have also been favoured at the chlorophyll *a* maximum by stronger upwelling over the canyon. Fernández and Bode (1991) interpreted east–west differences in microplankton composition in this area as a result of succession processes. The alongshore mesoscale physical forcing variability and its influence on primary production patterns (particularly in terms of size) suggest an additional cause for alongshore variation in microplankton composition.

Differences in the duration of life cycles result in a temporal delay in maximum mesozooplankton biomass relative to the spring phytoplankton bloom in temperate areas, which occurs in April in the Cantabrian Sea (Fernández and Bode, 1991). The enhancement of production by large-size phytoplankton coincides with a high abundance of crustacean mesozooplankton, dominated by copepods. Moreover, copepods are more abundant over the shelf, where large-size phytoplankton biomass and production dominate. This coupling enables high-energy flow through the food web to large metazoans (Legendre and Rassoulzadegan, 1996). High primary production related to a similar dome-shaped structure at the edge of the Avilés canyon in May (González-Quirós *et al.*, 2003) suggests persistence of this feature. Although the observed mesozooplankton distributions must be a consequence of processes affecting primary production earlier in the season and of advection from adjacent areas, there is a significant correlation with physical variables, which suggests some influence of the mesoscale dynamics on their distribution patterns.

Fish spawning patterns, reflected by egg distributions, may be interpreted as adaptive strategies that select favourable areas for larval development (Roy *et al.*, 1989). However, reproductive output in species with sequential (serial) reproduction, such as *S. pilchardus* and *S. scombrus*, will also depend on adult food availability during the spawning season, which to some extent may affect their spawning patterns. In the Cantabrian Sea, copepod developmental stages are the main prey of the diet of larvae of sardine (Conway *et al.*, 1994) and mackerel (I. Munera, Universidad de Oviedo, personal communication, from samples obtained during this survey). The diet of adult *S. pilchardus* in this area is composed of phytoplankton and zooplankton (Varela *et al.*, 1988). The spring diet of adult *S. scombrus* in this region consists of mesozooplankters (I. Olaso, Instituto Español de Oceanografía, personal communication). Therefore, it is difficult to differentiate between favourable conditions for larval stages and adult feeding. Nevertheless, the higher concentration and production of large phytoplankton over the shelf may concurrently enhance food availability for adult and larval stages. González-Quirós *et al.* (2003) observed high abundance of sardine, mackerel and horse mackerel eggs in this area related to high primary production at the southern edge of the Avilés canyon. High mean abundance of sardine larvae was observed in the area of the Avilés canyon from four cruises carried out in 1992 along the northwestern coast of the Iberian Peninsula (López-Jamar *et al.*, 1995). Our study provides evidence of predictable patterns of vertical instability related to topography and other mesoscale features that may benefit fish due to increased primary production and its transfer to higher trophic levels. High spawning intensity in this area may be interpreted as a response to favourable feeding conditions for larvae and/or adults.

Fernández *et al.* (1993) related the saline intrusion and the eastward circulation pattern to the entrapment of low salinity coastal waters on the shelf and the distribution of neritic zooplankton and ichthyoplankton. They argued that this hydrographic feature may play an important role for the transport of fish larvae and meroplanktonic larvae, thus influencing recruitment. In our study, sardine larvae were distributed further offshore than eggs, but not beyond the salinity front. Mackerel larvae presented a similar distribution to sardine larvae, but the egg distribution showed two distinct spawning areas, over the shelf and offshore. The observed larval distribution may be a consequence of an intense spawning activity that occurred previously in the coastal area. Walsh *et al.* (1996) suggested that poleward circulation along the western European shelf break causes the onshelf drift of mackerel larvae in the northern Bay of Biscay. This may also be the case along the Cantabrian Sea under dominant eastward circulation. In May 1995, distributions of sardine, mackerel and horse mackerel eggs and larvae in this area indicated onshelf retention in the absence of the saline intrusion but concurrent with the deepening of the isopycnals towards the coast and, thus, eastward transport (González-Quirós, 1999). The saline intrusion and the eastward circulation pattern may thus retain (*sensu* Sinclair, 1988) sardine and mackerel larvae in this area.

The saline intrusion was observed in May in 1987 (Botas *et al.*, 1989), 1994 (González-Quirós, 1999) and 1996 (González-Quirós *et al.*, 2003). Conversely, Gil *et al.* (2002) observed dominant westward geostrophic circulation in May 1995 and no along-slope, high-salinity nucleus. Monthly sampling of three stations in a single cross-shelf transect from 1993–2002 shows the presence of a nucleus of high salinity over the slope in May in 7 of 9 yr in this area (González-Quirós, unpublished data). The strength of the European slope current, which has been related to ecological regime shifts in the North Sea (Reid *et al.*, 2001), is proposed as an explanatory factor for the covariation between large-scale climatic indices and the biogeography of calanoid copepod assemblages over the European shelf (Beaugrand *et al.*, 2002). It can be expected that large-scale climatic forcing influences mesoscale processes associated with slope currents, and therefore the energy flow towards higher trophic levels and retention/advection of fish larvae.

In conclusion, mesoscale physical processes have been shown to affect the distribution of organisms and trophic pathways. Our study reveals predictable patterns of vertical instabilities that cause increased primary production dominated by large-size phytoplankton. Thus, taking into account the observed high mesozooplankton biomass dominated by copepods, high energy flow towards high trophic levels (fish) is expected. Spawning patterns of adult fish are associated with predictable features that benefit recruitment of their populations (van der Lingen and Huggett, 2003). Our study suggests that predictable vertical instabilities associated with slope currents may favour fish recruitment and be associated with their spawning patterns. The combined increase of energy flow to larval fish and their retention are hypothesized to be important to the dynamics of survival of early stages of *S. pilchardus* and *S. scombrus* in the Cantabrian Sea.

ACKNOWLEDGEMENTS

We thank the crew of the R/V *García del Cid*. We are indebted to José Pozo and Arturo Castellón (UTM) for their work with the CTD, other shipboard instruments and data management. We also thank the scientists and technicians from the *Universidad de Oviedo*, especially Leticia Viesca and Jorge Sostres for their work in phytoplankton production and nutrient analysis. Satellite images provided by Carlos García-Soto from the IEO (Santander Laboratory) were essential for planning the survey. A. Pascual held a doctoral fellowship from *Universitat de les Illes Balears*. This study and the contract held by R. González-Quirós were funded by the project 1FD97-1045-C02-01 [CICYT (Spanish Government) under the FEDER-EU program]. R.G.-Q. is especially grateful to Nines, Alejandro Gutiérrez-Bolívar and José García for their help on financial subsistence during the last phases of the writing of this manuscript. Suggestions by anonymous reviewers and the Editor significantly improved the final version. Moninya Roughan revised the English.

REFERENCES

Alvarez, A., Tintoré, J. and Sabatés, A. (1996) Flow modification of shelf-slope exchange induced by a submarine canyon off the northeast Spanish coast. *J. Geophys. Res.* **101:**12043–12055.

Beaugrand, G., Reid, P.C., Ibañez, F., Lindley, J.A. and Edwards, M. (2002) Reorganization of North Atlantic marine copepod biodiversity and climate. *Science* **296:**1692–1694.

Bode, A., Fernandez, E., Botas, A. and Anadon, R. (1990) Distribution and composition of suspended particulate matter related to a shelf-break saline intrusion in the Cantabrian Sea (Bay of Biscay). *Oceanol. Acta* **13:**219–228.

Botas, J. A., Fernández, E., Bode, A., Anadón, R. and Anadón, E. (1989) Datos básicos de las campañas 'COCACE': Hidrografía, nutrientes, fitoplancton y seston en el Cantábrico central. *Biobas. Rev. Biol. Univ. Oviedo.* **1:**78.

Bratseth, A.M. (1986) Statistical interpolation by means of successive correction. *Tellus* **38A:**439–447.

Checkley, D.M., Raman, S. Jr, Maillet, G.L. and Mason, K.M. (1988) Winter storm effects on the spawning and larval drift of a pelagic fish. *Nature* **335:**346–348.

Conway, D.V.P., Coombs, S.H., Fernández de Puelles, M.L. and Tranter, P.R.G. (1994) Feeding of larval sardine, *Sardina pilchardus* (Walbaum), off the north coast of Spain. *Bol. Inst. Esp. Oceanog.* **10:**165–175.

Cury, P. and Roy, C. (1989) Optimal environmental window and pelagic fish recruitment success in upwelling areas. *Can. J. Fish. Aquat. Sci.* **46:**670–680.

Cushing, D.H. (1975) *Marine Ecology and Fisheries*. Cambridge University Press, Cambridge, 278 pp.

Cushing, D.H. (1996) *Towards a Science of Recruitment in Fish Populations*. Ecology Institute, Oldendorf, 175 pp.

Denman, K.L. and Powell, T.M. (1984) Effects of physical processes on planktonic ecosystems in the coastal ocean. *Oceanogr. Mar. Biol. Ann. Rev.* **22:**125–168.

Fernández, E. and Bode, A. (1991) Seasonal patterns of primary production in the Central Cantabrian Sea (Bay of Biscay). *Sci. Mar.* **55:**629–636.

Fernández, E., Bode, A., Botas, A. and Anadón, R. (1991) Microplankton assemblages associated with saline fronts during a spring bloom in the central Cantabrian Sea: differences in trophic structure between water bodies. *J. Plankton Res.* **13:**1239–1256.

Fernández, E., Cabal, J., Acuña, J.L., Bode, A., Botas, A. and García-Soto, C. (1993) Plankton distribution across a slope current-induced front in the southern Bay of Biscay. *J. Plankton Res.* **15:**619–641.

Fortier, L., Levasseur, M.E., Drolet, R. and Therriault, J.C. (1992) Export production and the distribution of fish larvae and their prey in a coastal jet frontal region. *Mar. Ecol. Prog. Ser.* **85:**203–218.

Frouin, R., Fiuza, A.F.G., Ambar, I. and Boyd, T. (1990) Observations of a poleward surface current off the coasts of Portugal and Spain during winter. *J. Geophys. Res.* **95:**679–691.

Gil, J., Valdés, L., Moral, M., Sánchez, R. and García-Soto, C. (2002) Mesoscale variability in a high-resolution grid in the Cantabrian Sea (southern Bay of Biscay), May 1995. *Deep-Sea Res.* **49:**1591–1607.

González-Quirós, R. (1999) *Distribución del ictioplancton en el Cantábrico central y ecología alimentaria de Micromesistius poutassou* (Risso 1826). PhD thesis, Oviedo, Spain: Departamento de Biología de Organismos y Sistemas, Universidad de Oviedo, 217 pp.

González-Quirós, R., Cabal, J., Álvarez-Marqués, F. and Isla, A. (2003) Ichthyoplankton distribution and plankton production related to the shelf break front at the Avilés Canyon. *ICES J. Mar. Sci.* **60:**198–210.

Grasshoff, K., Ehrhardt, M. and Kremling, M. (1983) *Methods of Seawater Analysis*, 2nd edn. Weinheim: Verlag Chemie, 419 pp.

Haynes, R. and Barton, E.D. (1990) A poleward flow along the Atlantic coast of the Iberian Peninsula. *J. Geophys. Res.* **95:**11425–11441.

Hickey, B.M. (1995) Coastal submarine canyons. In: *Topographic Effects in the Ocean*. P. Müller & D. Henderson (eds). Proceedings 'Aha Huliko' a. Hawaiian Workshop, Manoa: University of Hawaii.

Hoskins, B.J., Draghici, I. and Davis, H.C. (1978) A new look at the omega-equation. *Quart. J. Roy. Met. Soc.* **104:**31–38.

Iles, T.D. and Sinclair, M. (1982) Atlantic herring: stock, discreteness and abundance. *Science* **215:**627–633.

Koutsicopoulos, C., Fortier, L. and Gagne, J.A. (1991) Cross-shelf dispersion of Dover sole (*Solea solea*) eggs and larvae in Bay of Biscay and recruitment to inshore nurseries. *J. Plankton Res.* **13:**923–945.

Le Fèvre, J. (1986) Aspects of the biology of frontal systems. *Adv. Mar. Biol.* **23:**163–299.

Le Fèvre, J. and Frontier, S. (1988) Influence of temporal characteristics of physical phenomena on plankton dynamics, as shown by North-West European marine ecosystems. In: *Toward a Theory on Biological–Physical Interactions in the World Ocean*. B.J. Rothchild (ed.) Dordrecht: Kluwer Academic Publishers, pp. 245–272.

Legendre, L. and Rassoulzadegan, F. (1996) Food-web mediated export of biogenic carbon in oceans: hydrodynamic control. *Mar. Ecol. Prog. Ser.* **145:**179–193.

van der Lingen, C.D. and Huggett, J.A. (2003) The role of ichthyoplankton surveys in recruitment research and management of South African anchovy and sardine. In: *The Fish Bang. Proceedings of the 26th Annual Larval Fish Conference*. H.I. Browman and A.B. Skiftesvik (eds) Bergen, Norway: Institute of Marine Research, pp. 303–344.

López-Jamar, E., Coombs, S.H., García, A., Halliday, N.C., Knust, R. and Nellen, W. (1995) The distribution and survival of larvae of sardine Sardina pilchardus (Walbaum, 1792) off the north and north-western Atlantic coast of the Iberian Peninsula, in relation to environmental conditions. *Bol. Inst. Esp. Oceanog.* **11:**27–46.

Munk, P., Larsson, P.O., Danielsen, D. and Moksness, E. (1995) Larval and small juvenile cod *Gadus morhua* concentrated in the highly productive areas of a shelf break front. *Mar. Ecol. Prog. Ser.* **125:**21–30.

New, A.L. and Pingree, R.D. (1990) Evidence for internal tidal mixing near the shelf break in the Bay of Biscay. *Deep-Sea Res.* **37:**1783–1803.

Pauly, D. and Chirstensen, V. (1995) Primary production required to sustain global fisheries. *Nature* **374:**255–257.

Pedder, M.A. (1993) Interpolation and filtering of spatial observations using successive corrections and Gaussian filters. *Mon. Wea. Res.* **121:**2889–2902.

Peterson, W. T., Arcos, D.F., McManus, G.B., Dan, H., Bellantoni, D., Johnson, T. and Tiselius, P. (1988) The nearshore zone during coastal upwelling: daily variability and coupling between primary and secondary production off central Chile. *Prog. Oceanog.* **20:**1–40.

Pingree, R.D. and Le Cann, B. (1990) Structure, strength and seasonality of the slope currents in the Bay of Biscay region. *J. Mar. Biol. Ass. UK* **70:**857–885.

Pingree, R.D., Mardell, G.T. and New, A.L. (1986) Propagation of internal tides from the upper slopes of the Bay of Biscay. *Nature* **321:**154–158.

Pinot, J.M., Tintoré, J. and Wang, D.P. (1996) A study of the omega equation for diagnosing vertical motions at ocean fronts. *J. Mar. Res.* **54:**239–259.

Reid, P.C., Holliday, N.P and Smyth, T.J. (2001) Pulses in the eastern margin current and warmer water off the north west European shelf linked to North Sea ecosystem changes. *Mar. Ecol. Prog. Ser.* **215:**283–287.

Roy, C., Cury, P., Fontana, A. and Belveze, H. (1989) Stratégies spatio-temporelles de la reproduction des clupéidés des zones d'upwelling d'Afrique de l'Ouest. *Aquat. Living Resour.* **2:**21–29.

Sabatés, A. and Masó, M. (1990) Effect of a shelf-slope front on the spatial distribution of mesopelagic fish larvae in the western Mediterranean. *Deep-Sea Res.* **37:**1085–1098.

Shea, R.E. and Broenkow, W.W. (1982) The role of internal tides in the nutrient enrichment of Monterey Bay, California. *Est. Coast. Shelf Sci.* **15:**57–66.

Sinclair, M. (1988) *Marine Populations: an Essay on Population Regulation and Speciation*. Seattle, WA: Washington Sea Grant Program, University of Washington Press, 252 pp.

Strickland, J.D.H. and Parsons, T.R. (1972) *A Practical Handbook of Seawater Analysis*, 2nd edn. Ottawa: Fisheries Research Board of Canada, 310 pp.

Varela, M., Larrañaga, A., Costas, E. and Rodríguez, B. (1988) El contenido estomacal de la sardina (*Sardina pilchardus* Walbaum) durante la campaña Saracus 871 en las plataformas Cantábrica y de Galicia en febrero de 1987. *Bol. Inst. Esp. Oceanog.* **5:**17–28.

Walsh, M., Skogen, M., Reid, D.G., Svensen, E. and McMillan, J.A. (1996) The relationship between the location of western mackerel spawning, larval drift and recruit distributions: a modelling study. *ICES (C.M. 1996/S)* **33:**35.

Wieters, E.A., Kaplan, D.M., Navarrete, S.A., Sotomayor, A., Largier, J., Nielson, K.J. and Véliz, F. (2003) Alougshore and temporal variability in chlorophyll *a* concentration in Chilean nearshore waters. *Mar. Ecol. Prog. Ser.* **249:**93–105.